Acoust. Sci. & Tech. **40**, 1 (2019)

PAPER

Role of the foot chamber in the sounding mechanism of a flue organ pipe

Shuhei Tateishi[1], Sho Iwagami[1], Genki Tsutsumi[1], Taizo Kobayashi[2,3], Toshiya Takami[4] and Kin'ya Takahashi[1,*]

[1]*Kyushu Institute of Technology, Kawazu 680–4, Iizuka, 820–8502 Japan*
[2]*Teikyo University, 6–22 Misaki-cho, Omuta, 836–8505 Japan*
[3]*Kyushu University, 744 Motooka, Nishi-ku, Fukuoka, 819–0395 Japan*
[4]*Oita University, 700 Dannoharu, Oita, 870–1192 Japan*

(*Received 18 May 2018, Accepted for publication 24 September 2018*)

Abstract: Two-demensional (2D) models of a flue organ pipe are studied with compressible fluid simulation, specifically compressible Large Eddy Simulation, focusing on the influence of the geometry of the flue and the foot on the jet motion and acoustic oscillation in the pipe. When the foot geometry is fixed, the models having a flue with chamfers show good performances in stabilizing the acoustic oscillation in the steady state. Furthermore, we find that the foot chamber works as a Helmholtz resonator. If the frequency of the acoustic oscillation in the pipe is higher than the resonance frequency of the Helmholtz resonator by almost the full-width at half-maximum, anti-phase synchronization between the acoustic oscillation in the pipe and that in the foot chamber occurs. In this case, the acoustic oscillation in the pipe grows rapidly in the attack transient and is stabilized in the steady state.

Keywords: Organ pipe, Organ foot, Helmholtz resonator

PACS number: 43.75.Np, 43.75.Qr, 43.75.Ef, 43.75.−z [doi:10.1250/ast.40.29]

1. INTRODUCTION

The study of the sounding mechanism of flue instruments, such as flute, recorder and flue organ pipe, is one of the long standing problems in the field of musical acoustics [1–3]. The relation between the frequency of acoustic oscillation and the jet velocity was first explained by Coltman using an equivalent circuit model based on experimental observations [4]. This was followed by Fletcher *et al.* where the relation was formulated in a clear way [1]. The oscillation phenomenon of the jet, which drives the resonance pipe, was studied by many authors [3,5–8]. Many aspects of the sounding mechanism have been clarified, such as the details of attack transient and the behavior of the jet motion changing with the jet velocity and the geometry of the mouth opening.

However, the sounding mechanism of flue instruments is still not understood completely. The major difficulty comes from the fact that the sound source of flue instruments, the edge tone, is aerodynamic sound that is caused by the unsteady motion of a fluid flow with non-zero vorticities [1,9]. The aerodynamic sound, which was first formulated by Lighthill, i.e., Lighthill's acoustic analogy, has attracted many authors' attention, but the generation mechanism of the aerodynamic sound has still not been completely elucidated [9,10]. Howe introduced an alternative method, Howe's energy corollary, which allows us to estimate the sound energy generation through the interaction between the fluid field and the acoustic field [9,11]. This is an indirect and approximate method, but is well applicable to some situations. Actually, the method to approximately calculate Howe's energy corollary has been recently developed in experiments of flue instruments by several authors [12,13]. As a result, it has been suggested that the aerodynamic sound is mainly generated from the jet downstream just before the edge. However, this needs to be confirmed by more rigorous methods, such as Lighthill's acoustic analogy.

On the other hand, in order to simultaneously calculate the jet motion and acoustic oscillation in the pipe, a numerical method with compressible fluid solvers has been recently developed by several authors [14–17]. This method well reproduces the detail behavior of the jet motion and acoustic oscillation, such as the change of the acoustic frequency with the jet velocity. Furthermore, it can be used for the calculation of Howe's energy corollary and gives essentially the same result as that obtained experimentally [18,19]. Therefore, numerical simulation

*e-mail: takahasi@mse.kyutech.ac.jp

based on a compressible fluid scheme is an important tool to explore the detail behavior of flue instruments.

In this paper, we focus on the problem of how the geometry of flue and foot chamber influences the jet motion and acoustic oscillation of a flue organ pipe. Ségoufin *et al.* experimentally studied the influence of the geometry of the flue with or without chamfers on the jet motion and acoustic oscillation for a flue organ pipe having a geometry typical of a recorder [8]. Their result indicates that shortening the flue allows better control of the instrument and makes the sound spectrum richer in high harmonics, while adding chamfers to the flue is effective in stabilizing oscillation only for a long flue but not for a short flue. In this paper, we numerically study a two-dimensional (2D) flue organ pipe model similar to that studied by Ségoufin *et al.* Furthermore, we investigate how the geometry of the foot chamber influences the stability of the jet motion and the acoustic oscillation in the pipe.

In this paper, we use a 2D flue organ pipe model instead of a three-dimensional (3D) model, because it is guaranteed that the basic properties of flue instruments, e.g., the relation between the acoustic frequency and the jet velocity, are well reproduced by using a 2D model [14,18]. The advantage of using the 2D model is that it can be calculated with less computer power and less resources. The simulation of 3D models with a compressible fluid scheme, that is a compressible Large Eddy Simulation (LES), is a very heavy task [14,20] and to study the functions of the flue and the foot chamber we have to execute many simulations of many models with different shapes.

2. SOUNDING MECHANISM OF ORGAN PIPE

2.1. Sound Source: Edge Tone

As shown in Fig. 1, a jet injected from a flue collides with an edge (labium) and causes vortices. The reaction of vortices influences the jet to oscillate in the vertical direction. The aerodynamic sound, known as edge tone, is created by the oscillating jet together with the vortices [9].

The relation between the oscillation frequency f of the edge tone and the jet velocity V is given by Brown's equation [21],

$$f = 0.466 j_k (100V - 40)(1/100l - 0.07), \qquad (1)$$

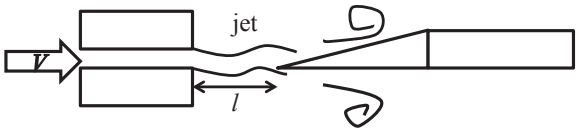

Fig. 1 Generation of edge tone.

where l denotes the distance between the flue exit and the edge. The variables f, V and l are in SI units so that the units of the constants are 40 m/s and 0.07 m^{-1}. The unit of frequency f is the hertz (Hz). The parameter j_k changes with the oscillation mode of the jet and has values $j_1 = 1.0$, $j_2 = 2.3$, $j_3 = 3.8$ and $j_4 = 5.4$. For flue instruments, the first hydrodynamic mode with $j_1 = 1.0$ is usually observed and the frequency f increases linearly with the jet velocity V.

2.2. Sounding Mechanism of Flue Organ Pipe

The edge tone generated by the jet oscillation drives the resonance pipe, and cooperative behavior of the jet motion and the acoustic modes of the pipe makes the sound of the organ pipe [1,14]. According to Coltman, the relation between the dominant sound frequency and the jet velocity for a closed end pipe is as shown by the thick lines in Fig. 2 [4]. First, the sound frequency increases linearly with the jet velocity just as the frequency of the edge tone does. Then, just before the sound frequency reaches the first resonance frequency of the pipe, the increase rate decreases and the sound frequency converges to the pipe resonance frequency with increasing jet velocity. Here, the jet motion becomes synchronized with the first acoustic mode, which makes a sound with a clear pitch. As the jet velocity increases further, the edge tone frequency increases, the synchronization becomes incomplete, and the sound is a blended composite of the dominant pipe tone and the edge tone. At higher values of jet velocity, where the edge tone frequency of Eq. (1) approaches the second pipe resonance frequency, the jet motion changes and starts to be synchronized with the second pipe mode. Here, the second mode dominates the fundamental mode and the dominant frequency of the acoustic wave jumps to the second pipe resonance frequency.

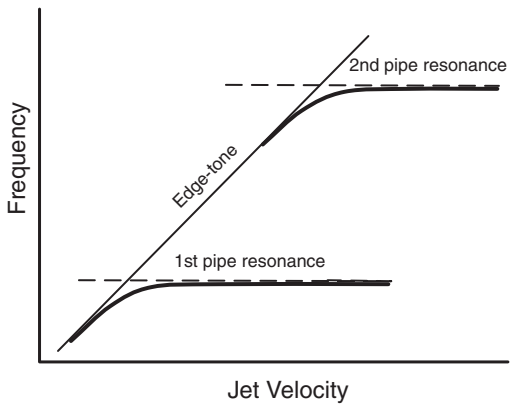

Fig. 2 Oscillation frequency vs. jet velocity for a closed end pipe.

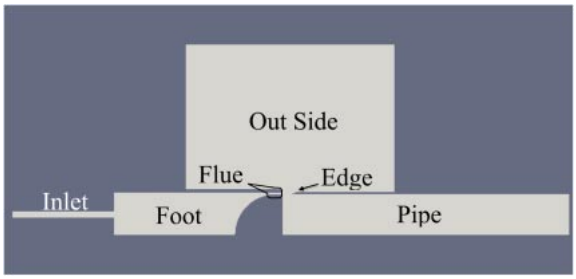

Fig. 3 Geometry of the 2D flue organ pipe model with an inlet tube, a foot chamber, a flue and a resonance pipe with a closed end. The particular case of the Reference foot and the short flue with chamfers is shown.

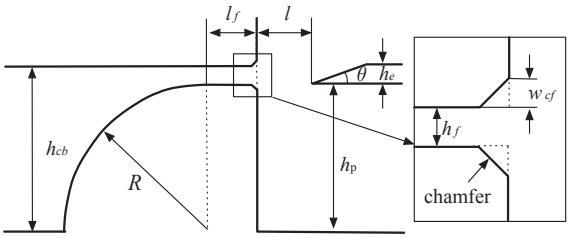

Fig. 4 Dimensions of the edge, flue with chamfers and foot channel: $h_p = 20\,\text{mm}$, $l = 4\,\text{mm}$, $h_e = 1.2\,\text{mm}$, $\theta = 20^\circ$, $w_{cf} = 0.71\,\text{mm}$, $h_f = 1\,\text{mm}$, $l_f = 3$ or $15\,\text{mm}$, $h_{cb} = 20.8\,\text{mm}$, $R = 19.8\,\text{mm}$.

3. MODEL AND NUMERICAL METHOD

3.1. Model

In this paper, we analyze a 2D model of a flue organ pipe with a closed end, which is a 2D analog of the organ pipe studied by Ségoufin *et al.* [8]. As shown in Fig. 3, the model consists of an inlet tube, a foot chamber, a flue and a resonance pipe. The volume above the flue and edge models the outside space with the external atmosphere.

The pipe is 141.5 mm in length and the frequency of the fundamental resonance mode is estimated as 583 Hz taking into account the 2D end correction at the mouth opening [14]. The pipe length of our model is half as long as that studied by Ségoufin *et al.* [8]. We adopt the closed pipe, while Ségoufin *et al.* studied the open pipe, so the fundamental frequencies are almost the same in the two models. Note that the pipe is 20 mm in height.

The distance between the flue exit and the top of the edge is set as $l = 4\,\text{mm}$ and the flue is 1 mm in height (see Fig. 4). The intersection of Brown's equation given by Eq. (1) at $j_1 = 1$ with the fundamental resonance frequency gives the jet velocity of $V \approx 5.6\,\text{m/s}$. According to the Coltman-Fletcher theory [1,4], the optimal oscillation is at the jet velocity slightly above the intersection point, and so we set the desired average jet velocity to be $V = 6\,\text{m/s}$. The height of the inlet tube is 3 mm, which is three times as large as the height of the flue, and the flow velocity at the inlet should be set as one third of the desired jet velocity. Note that the length of the inlet tube is 50 mm.

Table 1 Abbreviations of the flue models.

flue length	with chamfers	without chamfers
short: 3 mm	SC	SE
long: 15 mm	LC	LE

As in Ségoufin *et al.* [8], we investigate the changes of the jet motion and acoustic oscillation with the geometry of the flue. To do this, we adopt four types of flues, with short or long channel, i.e., 3 mm or 15 mm in length, and with or without chamfers at the flue exit. The dimensions of the flue and chamfers are given in Fig. 4. As shown in Table 1 we call the short flue models with and without chamfers the SC and SE models, respectively, and call the long flue models with and without chamfers the LC and LE models, respectively.

We also investigate the role of the foot chamber, considering how the geometry and volume of the foot chamber influences the jet motion and acoustic oscillation. The models used for this investigation are different to each other in the foot geometry but have the same short flue with chamfers, because, as shown later, the SC model shows the best performance in making the attack transient short and stabilizing the acoustic oscillation in the steady state. Figure 5 shows the geometry of the foot models and Table 2 shows their abbreviations. As shown in Figs. 4 and 5, the foot chamber consists of the left rectangular part and the right channel part, which gradually narrows toward the flue channel and is smoothly connected to it. The lower channel block below the channel is a quarter circle.

The foot chamber shown in Fig. 5(a) is the same as that of the model in Fig. 3. As shown in Table 2, the foot chamber in Fig. 5(a) is called the Reference model or the Reference foot. The rectangular part of the Reference model is 60 mm in length and 20.8 mm in height. We also investigate three different-shaped foot models, the Short, Long and Isovolume models. For the Short and Long models in Figs. 5(b) and (c), the rectangular parts are 30 mm and 120 mm in length, respectively. For the Isovolume model in Fig. 5(d), the rectangular part is 30 mm in length and 41.6 mm in height and it has the same 2D volume as the Reference model. Furthermore, we also investigate a model without the foot chamber and inlet tube, which is called the Non-foot model.

3.2. Numerical Method

For the numerical calculation, we adopt a compressible LES (Large Eddy Simulation) solver in the open source software, *OpenFOAM* ver.2.2.2 [14,18]. Specifically, we

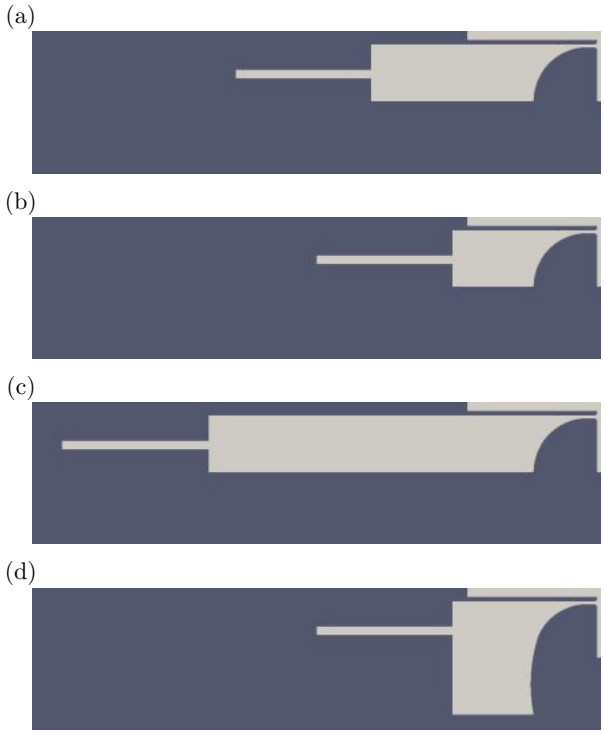

Fig. 5 Geometry of the foot chamber. (a) Reference model. (b) Short model. (c) Long model. (d) Isovolume model.

Table 2 Abbreviations of the foot models.

abbreviation	foot geometry
Reference	Fig. 5(a)
Short	Fig. 5(b)
Long	Fig. 5(c)
Isovolume	Fig. 5(d)
Non-Foot	without the foot and inlet tube

use the scheme called 'rhoPisoFoam' with the one-equation sub-grid-scale (SGS) model, which is suitable for fluid at subsonic speeds. The pressure and temperature in the atmosphere at rest are take as $p_0 = 100\,\mathrm{kPa}$ and $T_0 = 300\,\mathrm{K}$, respectively. To guarantee numerical accuracy, the size of the mesh around the mouth opening is $\Delta x = 0.1$ mm and the time step of the numerical integration is $\Delta t = 5.0 \times 10^{-8}$ s. In the case of the model in Fig. 3, for example, with the Reference foot and the short flue with chamfers, the number of mesh cells is 120165.

The outlet boundary condition is taken for the right, left and top walls of the volume above the instrument. The inlet boundary condition is taken for the left end of the inlet tube. The other walls are solid walls. The flow velocity at the inlet is initially increased gradually to reach the desired value at $t = 2\,\mathrm{ms}$. The time evolution up to 50 ms is calculated. Note that in *OpenFOAM* the inlet boundary behaves as a diode, that is, it becomes a transparent wall for an incoming flow, but a solid wall for an outgoing flow.

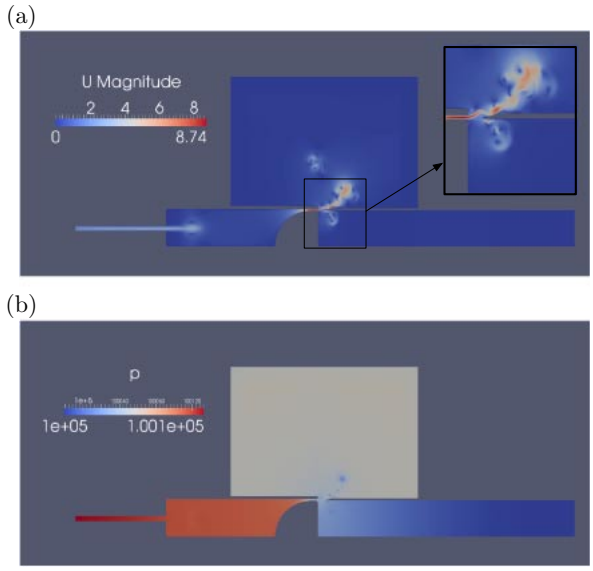

Fig. 6 Snapshots of spatial distributions of velocity and pressure for the SC model with the Reference foot. (a) Velocity distribution. (b) Pressure distribution.

Thus, the foot chamber and the inlet tube behave as a cavity.

The pressure oscillations in the pipe and in the foot chamber are observed at the center of the right end of the pipe and at the upper-left point of the rectangular part of the foot, respectively. The jet velocity is observed at the center of the flue exit.

4. NUMERICAL RESULTS

4.1. Velocity and Pressure Distribution of the SC Model with the Reference Foot

Figure 6 shows the snapshots of spatial distributions of velocity and pressure in the steady state for the SC model with the Reference foot, which provides the most stable oscillation among the SC, SE, LC and LE models. As shown in Fig. 6(a), the jet spontaneously oscillates, colliding with the edge and emitting the edge tone, which drives the resonance pipe. As shown in Fig. 6(b), the acoustic pressure oscillation with the frequency 482 Hz is well sustained in the resonance pipe. Note that, as shown to be normal in Fig. 2, the oscillation frequency in the steady state is smaller than the resonance frequency of the pipe obtained theoretically: 482 Hz (observation) $<$ 583 Hz (theory). Furthermore, the pressure in the foot chamber oscillates in anti-phase with that in the pipe. As will be shown in the following subsections, this anti-phase synchronization is the key for understanding the role of the foot chamber.

4.2. Results of the SC, SE, LC and LE Models with the Reference Foot

In this subsection we consider the pressure oscillation

Table 3 Evaluation of the models.

	SC	SE	LC	LE
Attack	Good	Fair	Fair	Poor
Steady state	Good	Fair	Good	Fair

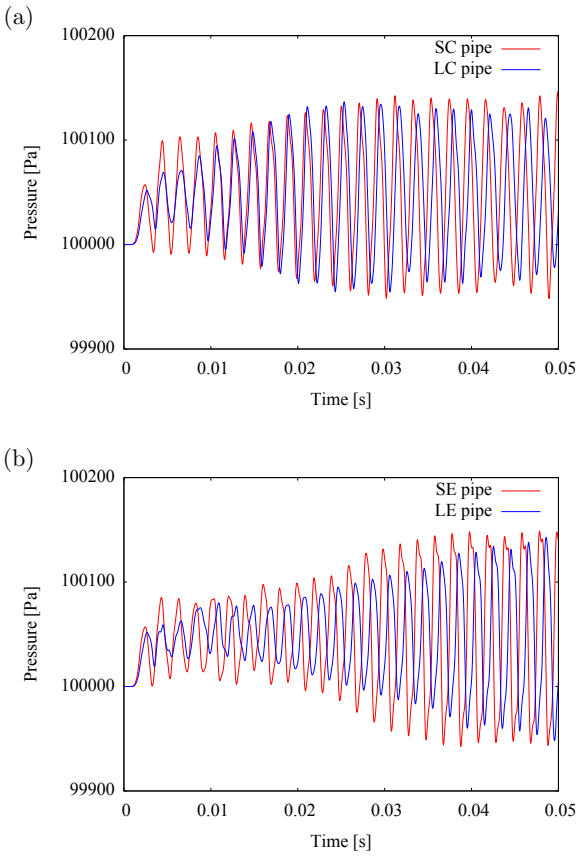

Fig. 7 Time evolution of the pressure in the pipe. (a) SC and LC models. (b) SE and LE models.

observed at the center of the right end of the pipe. In particular, we focus on the following features:

1) Attack: Brevity of attack transient;
2) Steady-state: Stability and size of oscillation amplitude.

Our subjective evaluations ("good," "fair," or "poor") for the four models are shown in Table 3.

Let us describe details. Figure 7(a) shows the pressure oscillations in the pipe for the SC and LC models and Fig. 7(b) shows those for the SE and LE models. The maximum amplitude of the pressure oscillation reaches around 100 Pa for all the models. However, the behavior of the models with chamfers, the SC and LC models, is different from that of the models without chamfers, the SE and LE models.

For the SC and LC models, the oscillations are dominated by the fundamental mode and their wave forms are similar to a sinusoidal wave in the steady state. The

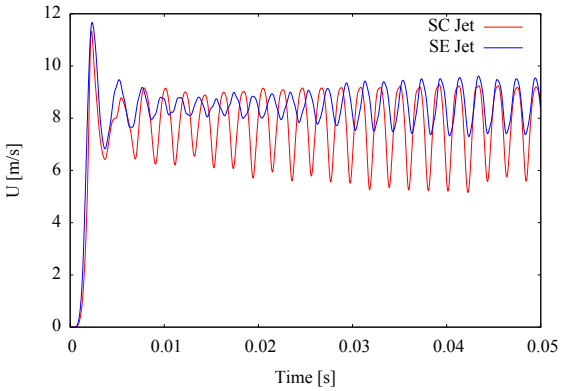

Fig. 8 Time evolution of the horizontal velocity at the flue exit for the SC and SE models.

attack transient of the SC model is short and the oscillation amplitude reaches around 50 Pa at $t = 5$ ms. On the other hand, for the LC model, the oscillation amplitude monotonically increases until 25 ms and it does not have a definite attack transient.

For the SE and LE models, the oscillations have small amplitude until 20 ms and gradually grow after that. In the initial stage until 20 ms, the oscillations are rather unstable and seem to be modulated by high frequency components. In this stage, oscillation amplitude for the LE model is smaller and more unstable than that for the SE model. In the later stage, the wave forms are still different from sinusoidal waves due to higher harmonic components. The LE model takes a longer time to reach the maximum oscillation than the SE model.

The above results show that the models with chamfers are more stable than the models without chamfers. Figure 8 shows the time evolution of horizontal velocity at the flue exit for the SC and SE models. The velocity of the SC model periodically oscillates in the steady state at the same frequency as the acoustic oscillation. On the other hand, the velocity of the SE model is rather unstable and has small amplitude until 20 ms. Even in the later stage, it has smaller amplitude than the SC model. The oscillation of the horizontal velocity of the jet probably helps to stabilize the acoustic oscillation.

Our numerical results show that the models having the flue with chamfers, i.e., the SC and LC models, show good performance in obtaining stable and large-amplitude oscillation in the steady state. Furthermore, the SC model is shorter in the attack transient than the LC model. Thus, our numerical results partially agree with the experimental results by Ségoufin *et al.* [8]. Indeed, they indicated that adding chamfers to a long flue is effective in stabilizing the system and makes the attack transient less abrupt. The result for the LC and LE models is similar to their result, except for the ambiguous attack transient of the LE model. However, they indicated that adding chamfers to a short

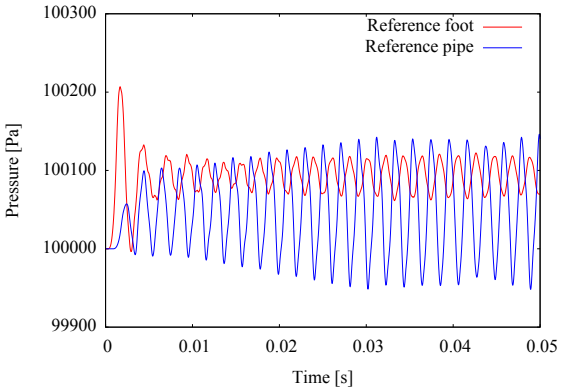

Fig. 9 Time evolution of the pressure in the pipe and that of the pressure in the foot chamber for the Reference foot model (with the SC flue model).

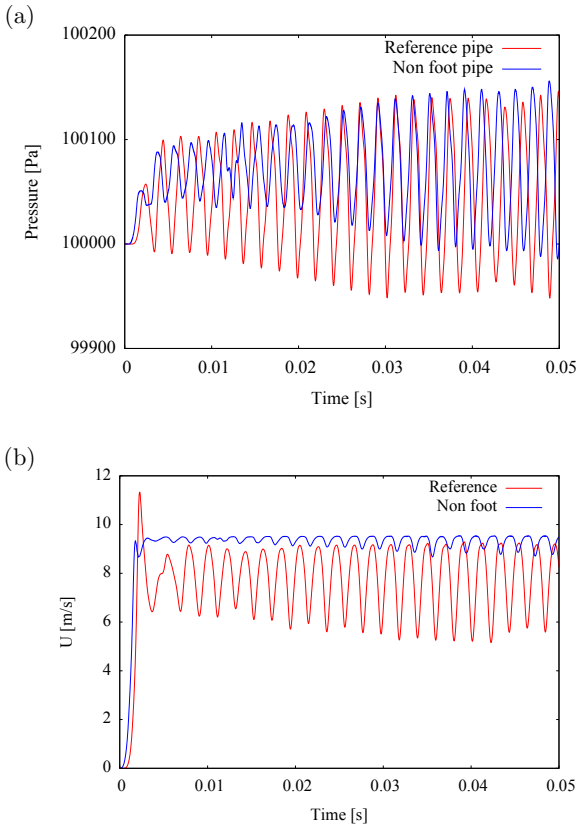

Fig. 10 Comparison between the Reference model and the Non-foot model. (a) Pressure in the pipe. (b) Jet velocity at the flue exit.

flue does not help to stabilize the system, while our result shows that the SC model is more stable than the SE model. This disagreement is attributed to the difference in the shape of the foot chambers. To make the flue short, Ségoufin *et al.* replaced the lower channel block with a different-shaped one, a triangle-shaped block. On the other hand, our models have the same channel block, i.e., the quarter circle block. As shown in Appendix, the numerical simulation for the 2D models of the short flue organ pipe with and without chamfers studied by Ségoufin *et al.* is qualitatively in agreement with their experimental result. Therefore, it is considered that the replacement of the lower channel block not only changes the geometry and volume of the foot chamber but also affects the formation of the jet and the interaction between the foot chamber and resonance pipe through the flue. In the following, we explore the role of the foot chamber.

4.3. Interaction between the Resonance Pipe and the Foot Chamber

In this subsection, we consider the interaction between the resonance pipe and the foot chamber. We use the Reference model and the short flue with chamfers, i.e., the SC model, which shows the best performance as described in Sect. 4.2.

Figure 9 shows the time evolution of the acoustic pressure in the pipe compared with that in the foot chamber. In the steady state, anti-phase synchronization between the pressure oscillation in the pipe and that in the foot chamber is observed. Indeed, one lags behind or leads the other in phase by nearly π, because of the interaction between the resonance pipe and the foot chamber through the flue. Comparing with Fig. 8, we find that the oscillation of the horizontal velocity of the jet leads the pressure oscillation in the pipe by nearly $\pi/2$ and lags behind the pressure oscillation in the foot chamber by nearly $\pi/2$. It seems that the anti-phase synchronization adds a small periodical oscillation on the jet velocity, which stabilizes the motion of the coupled system of the pipe and the foot chamber.

4.4. Comparison between the Reference Model and the Non-foot Model

To explore the role of the foot chamber, we compare the model with the Reference foot, i.e., the Reference foot model, with the model without the foot chamber and inlet tube, i.e., the Non-foot model, for which the air flow is directly injected from the left end of the flue. Note that both models have the same short flue with chamfers, i.e. the SC flue model. Figures 10(a) and (b) show the time evolution of the acoustic pressure in the pipe and that of the horizontal velocity at the flue exit for these two models, respectively. The pressure oscillation for the Non-foot model is unstable until $t = 20$ ms and gradually increases until $t = 50$ ms. In this sense, it has a long attack transient. Even at $t = 50$ ms, its amplitude is still smaller than that of the Reference model. The oscillation of the velocity at the flue exit for the Non-foot model gradually grows, but its amplitude is much smaller than that of the Reference model even at $t = 50$ ms. Thus, there is an interaction between the pipe and foot chamber for the Reference model and the

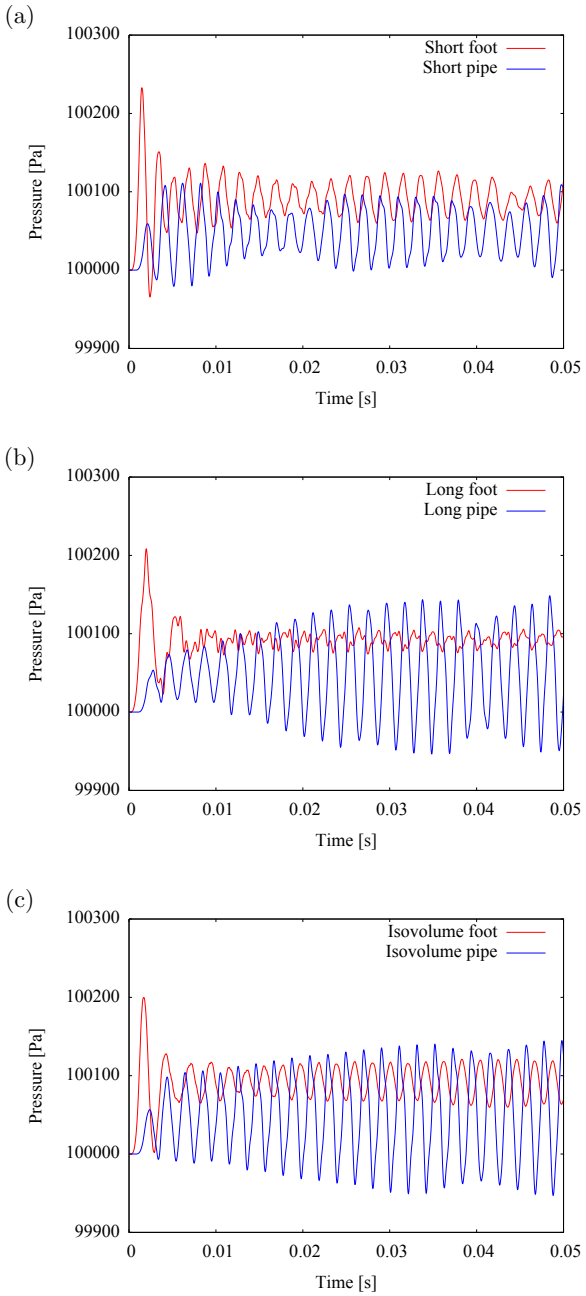

Fig. 11 Pressure in the foot chamber and that in the pipe. (a) Short model. (b) Long model. (c) Isovolume model.

existence of the foot chamber assists the acoustic oscillation to grow rapidly.

4.5. The Role of the Foot Chamber

To clarify the role of the foot chamber, we study the four models whose foot chambers are different in geometry to each other: the Reference, Short, Long and Isovolume models in Fig. 5. Note that the four models have the same short flue with chamfers, i.e., the SC model.

Figure 11(a) shows the result of the Short model. The attack transient of the acoustic pressure in the pipe is as short as that of the Reference model in Fig. 9. In the steady state, the oscillation amplitude is smaller than that of the Reference model and gradually fluctuates as a beat sound wave. The pressure oscillation in the foot chamber also behaves as a beat sound wave but with a slightly different frequency from that of the acoustic oscillation in the pipe. The pressure oscillations in the foot chamber and the pipe are not in synchronization or anti-phase synchronization. Most of the time, the pressure oscillation in the foot chamber lags behind that in the pipe by nearly $\pi/2$.

Figure 11(b) shows the result of the Long model. The acoustic pressure in the pipe has a long attack transient and gradually grows until it reaches the maximum amplitude. Even in the steady state, the acoustic oscillation is rather unstable compared with that of the Reference model. In the first stage of time evolution, the pressure oscillation in the foot chamber fluctuates irregularly and there is not clear synchronization or anti-phase synchronization between the pressure oscillation in the foot chamber and that in the pipe, but they seem to fall into anti-phase synchronization after a long time.

Figure 11(c) shows the result of the Isovolume model. The time evolution of the acoustic pressure in the pipe almost coincides with that of the Reference model. Furthermore, anti-phase synchronization between the acoustic oscillation in the pipe and that in the foot chamber is observed in the steady state. This means that the function of the foot chamber of the Isovolume model is the same as that of the Reference model.

These results show that the function of the foot chamber depends only on its volume and not on its shape. From this observation, it is expected that the foot chamber works as a Helmholtz resonator. In the following, we consider how the foot chamber works as a Helmholtz resonator, the origin of the phase difference between the oscillations in the foot chamber and the pipe, and its relation to the amplitude and stability of the acoustic oscillations.

The oscillation frequency of a Helmholtz resonator f_{H} is given by [1]

$$f_{\mathrm{H}} = \frac{c}{2\pi}\sqrt{\frac{S}{V_{\mathrm{H}}L}}, \tag{2}$$

where c is the speed of sound in air, S is the cross section of the neck, L is the length of the neck and V_{H} is the volume of air in the resonator's body. Note that, for the 2D model, S and V_{H} are the height of the neck and the 2D area of the foot chamber, respectively. To consider the relation to the 3D model we can add a uniform width w perpendicular to the 2D model geometry. Thus the cross section of the neck and the volume of the air in the resonator's body for the 3D model are $S \times w$ and $V_{\mathrm{H}} \times w$, respectively. From Eq. (2), the 2D and 3D models have the same resonance frequency.

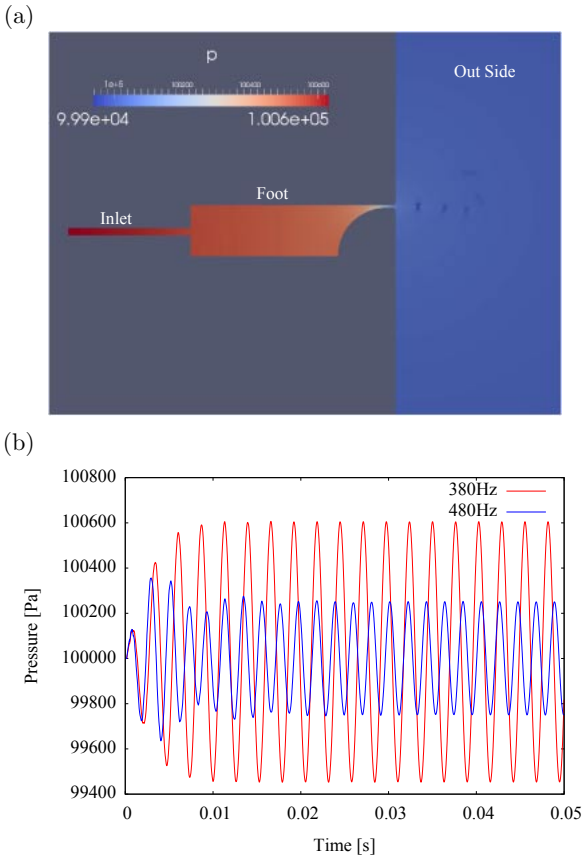

Fig. 12 Pressure in the Helmholtz resonator of the Reference model. (a) Snapshot of the pressure distribution at $f = 380\,\mathrm{Hz}$. (b) Pressure at the upper-left point of the rectangular part of the foot at $f = 380$ and 480 Hz.

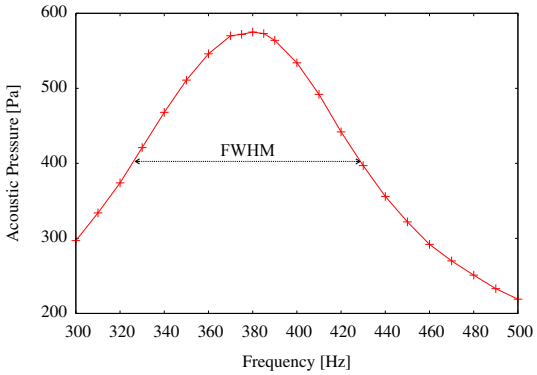

Fig. 13 Frequency response of the Helmholtz resonator of the Reference model. The dotted line with arrows labeled 'FWHM' indicates the value of $1/\sqrt{2}$ times the maximum.

Table 4 Helmholtz frequency f_H compared with the frequency of the acoustic oscillation f_a for the representative models.

	Reference	Short	Long	Isovolume	LC
f_H [Hz]	380 ± 5	495 ± 5	265 ± 5	385 ± 5	270 ± 5
f_a [Hz]	482	481	479	482	473

Roughly speaking, the foot chamber and flue play the role of the resonator's body and that of the neck, respectively. However, we do not have a method to determine the boundary between the resonator's body and neck for such a complex-shaped resonator. As an alternative method, we numerically obtain the resonance frequency of the foot chamber separated from the pipe. Here, we use the compressible LES solver for the calculation.

Figure 12(a) shows the Helmholtz resonator of the Reference model, which is formed by the flue and foot chamber connected to the inlet tube. The area of the outside section on the right is $500 \times 500\,\mathrm{mm}^2$. To consider the frequency response of the Helmholtz resonator, the flow velocity at the inlet U_in is changed periodically as

$$U_\mathrm{in}(t) = U_0 \sin(\omega t), \tag{3}$$

where the amplitude U_0 is set as $U_0 = 1\,\mathrm{m/s}$.

Figure 12(a) shows a snapshot of the pressure distribution at $f = 380\,\mathrm{Hz}$ and Fig. 12(b) shows the time evolution of the pressure at the upper-left point of the rectangular part of the foot at $f = 380$ and 480 Hz. Stable oscillations are observed in the stationary states at $f = 380$ and 480 Hz. The amplitude of the pressure oscillation at $f = 380\,\mathrm{Hz}$ is more than twice as large as that at $f = 480\,\mathrm{Hz}$, which is almost the frequency of the acoustic oscillation of the pipe $f_\mathrm{a} = 482\,\mathrm{Hz}$. Figure 13 shows the frequency response of the amplitude of acoustic pressure p_ap in the foot chamber. A resonance peak exists at $f = 380 \pm 5\,\mathrm{Hz}$ and the peak height is 575 Pa. The amplitude p_ap takes the value of $1/\sqrt{2}$ times the maximum, i.e., half the maximum of the acoustic intensity, at $f \approx 327\,\mathrm{Hz}$ and $f \approx 428\,\mathrm{Hz}$. Thus, the full-width at half maximum (FWHM) is approximately 100 Hz, and the frequency of the acoustic oscillation $f_\mathrm{a} = 482\,\mathrm{Hz}$ is higher than the Helmholtz resonance frequency $f_\mathrm{H} \approx 380\,\mathrm{Hz}$ by nearly the FWHM value.

Table 4 shows the Helmholtz resonance frequency f_H compared with the frequency of the acoustic oscillation f_a for the representative models. For the Isovolume model, $f_\mathrm{H} = 385 \pm 5\,\mathrm{Hz}$, which is close to that for the Reference model. This means that the functions of the foot chamber for the Reference and Isovolume models are almost the same. For the Short model, $f_\mathrm{H} = 495 \pm 5\,\mathrm{Hz}$, which is slightly higher than the oscillation frequency at $f_\mathrm{a} = 481$ Hz. In this case, unstable oscillations with relatively small amplitude arise in the pipe and foot chamber (see Fig. 11). For the Long model and the LC model, i.e., the Reference model with the long flue with chamfers, the Helmholtz

frequencies are $265 \pm 5\,\mathrm{Hz}$ and $270 \pm 5\,\mathrm{Hz}$, which are much less than those of acoustic oscillations at $f_a = 479$ and 482 Hz, respectively. In this case, pressure fluctuation in the foot chamber does not become larger and the acoustic oscillation in the pipe does not grow rapidly (see Fig. 11).

In the steady state, the phase difference between the pressure oscillation in the pipe and that in the foot chamber can be explained by the theory of forced harmonic oscillators (TFHO). This means that the acoustic oscillation in the pipe drives the Helmholtz resonator, i.e., the foot chamber.

According to TFHO, if the frequency of the acoustic oscillation is higher than the Helmholtz resonator frequency by almost the FWHM value, the phase of the Helmholtz resonance oscillation should lag behind that of the acoustic oscillation by almost π, because the foot chamber, i.e., the Helmholtz resonator, is driven in the mass dominated region. This is consistent with the observation of anti-phase synchronization in the simulation. However, TFHO can not explain the fact that the acoustic oscillation in the pipe rapidly grows in the attack transient and is stabilized in the steady state. Explaining this would require a more detailed analysis of the mechanism of the jet motion coupled with oscillations in the pipe and the boot chamber.

When the frequency of the acoustic oscillation is much higher than the Helmholtz resonance frequency as in the Long model and LC model, i.e., the mass dominated region, the pressure oscillation in the foot chamber has a very small amplitude, even though anti-phase synchronization occurs. In this case, the system rather behaves like the Non-foot model, namely the rapid growth of the acoustic oscillation is not observed (compare Fig. 7(a) and Fig. 11(b) with Fig. 10(a)). This behavior is consistent with the TFHO for when the frequency of the driving oscillation is far from the resonance frequency of the driven oscillator.

If the frequency of the pipe is close to the Helmholtz resonance frequency, the phase of the Helmholtz oscillation lags behind that of the acoustic oscillation in the pipe by almost $\pi/2$. This is also consistent with the resonant response predicted by the TFHO applied to the resistance dominated region. However, the pressure oscillations observed in the foot chamber and the pipe are unstable and have relatively small amplitude. This cannot be explained by the TFHO. We conjecture that energy transfer between the pipe and foot chamber enhanced by resonant interaction may destabilize the system, and that hydrodynamic interaction should play a role, i.e., the oscillating jet and aerodynamic sound generated by it. To clarify this we need to do further investigation of the interaction among the oscillation in the foot chamber, the jet motion and the oscillation in the pipe.

5. DISCUSSION

In this paper, we numerically studied the 2D flue organ pipe model with a foot chamber, focusing on the problem of how the geometries of the flue and the foot chamber influence the acoustic oscillation in the pipe.

First, we investigated the changes of the jet motion and acoustic oscillation with the geometry of the flue, when the geometry of the foot is fixed. Specifically, we studied four flue models, i.e., the SC, SE, LC and LE models, with either a short or a long flue, and with or without chamfers. As a result, it was found that the models having a flue with chamfers, i.e., the SC and LC models, show good performance in stabilizing the acoustic oscillation in the steady state. Furthermore it was found that the SC model with the short flue has shorter attack transient than the LC model with the long flue.

Next, we explored the function of the foot chamber comparing the Reference foot model, with the SC flue model, with three models which have a different shaped foot chamber. As a result, it was found that the function of the foot chamber depends on its volume and it acts as a Helmholtz resonator. Frequency and phase relations indicate that the acoustic oscillation in the pipe drives the oscillation in the Helmholtz resonator. When the frequency of the acoustic oscillation is higher than that of the Helmholtz resonator by almost the resonator's FWHM, anti-phase synchronization between the acoustic oscillation in the pipe and that in the foot chamber occurs. In this case, the acoustic oscillation grows rapidly in the attack transient and is stabilized in the steady state. However, if the frequency of the acoustic oscillation is nearly equal to that of the Helmholtz resonator, the acoustic oscillation in the pipe and that in the foot chamber become small and unstable, even though a resonance is expected from the theory of forced harmonic oscillators. On the other hand, when the frequency of the acoustic oscillation is much higher than that of the Helmholtz resonator, namely the frequency of the driving oscillation is far from the resonance peak, anti-phase synchronization occurs but the pressure oscillation in the foot chamber has a very small amplitude and rapid growth of the acoustic oscillation is not observed.

We have shown how the detuning of the pipe acoustic oscillation frequency from the Helmholtz resonance frequency affects the phase difference between the acoustic oscillations in the pipe and the pressure oscillation in the foot chamber, and the amplitude and stability of the acoustic oscillations. To understand the mechanisms of growth and stabilization we need to further investigate the nonlinear interactions among the oscillation in the foot chamber, the jet motion and the oscillation in the pipe. Our result shows that optimally the frequency of the acoustic

oscillation in the pipe should be higher than the Helmholtz resonance frequency of the foot chamber by almost the full-width at half-maximum. This point should be taken into account for the design of the flue organ pipe. To clarify this point, we have to investigate the function of the foot chamber in more detail with calculations of 3D models. This task is left for future work. It should also be checked by experiments.

ACKNOWLEDGMENT

The present work was supported by a Grant-in-Aid for Scientific Research (C) No. 16K05477 from the Japan Society for the Promotion of Science (JSPS) and by "Joint Usage/Research Center for Interdisciplinary Large-scale Information Infrastructures" in Japan (Project ID: jh170021-NAJ, jh180007-MDH).

REFERENCES

[1] N. H. Fletcher and T. D. Rossing, *The Physics of Musical Instruments*, 2nd ed. (Springer-Verlag, New York, 1998).
[2] A. Hirschberg, "Aero-acoustics of wind instruments" in *Mechanics of Musical Instruments*, A. Hirschberg, J. Kergomard and G. Weinreich, Eds. (Springer-Verlag, Vienna/New York, 1995), pp. 291–369.
[3] B. Fabre, J. Gilbert, A. Hirschberg and X. Pelorson, "Aeroacoustics of musical instruments," *Annu. Rev. Fluid Mech.*, **44**, 1–25 (2011).
[4] J. W. Coltman, "Jet driven mechanisms in edge tones and organ pipes," *J. Acoust. Soc. Am.*, **60**, 725–733 (1976).
[5] B. Fabre, A. Hirschberg and A. P. J. Wijnands, "Vortex shedding in steady oscillation of a flue organ pipe," *Acta Acust. united Ac.*, **82**, 863–877 (1996).
[6] S. Yoshikawa, "Jet-wave amplification in organ pipes," *J. Acoust. Soc. Am.*, **103**, 2706–2717 (1998).
[7] S. Yoshikawa, "A pictorial analysis of jet and vortex behaviours during attack transients in organ pipe models," *Acta Acust. united Ac.*, **86**, 623–633 (2000).
[8] C. Ségoufin, B. Fabre, M. P. Verge, A. Hirschberg and A. P. J. Wijnands, "Experimental study of the influence of the mouth geometry on sound production in a recorder-like instrument: windway length and chamfers," *Acta Acust. united Ac.*, **86**, 649–661 (2000).
[9] M. S. Howe, *Acoustics of Fluid-Structure Interactions* (Cambridge University Press, Cambridge, 1998).
[10] M. J. Lighthill, "On sound generated aerodynamically I. General theory," *Proc. R. Soc. Lond. A*, **A211**, 564–587 (1952).
[11] M. S. Howe, "On the absorption of sound by turbulence and other hydrodynamic flows," *IMA J. Appl. Math.*, **32**, 187–209 (1984).
[12] A. Bamberger, "Vortex sound in flutes using flow determination with endo-piv," *Forum Acusticum Budapest 2005, 4th European Congress on Acoustics*, pp. 665–670 (2005).
[13] S. Yoshikawa, H. Tashiro and Y. Sakamoto, "Experimental examination of vortex-sound generation in an organ pipe: A proposal of jet vortex-layer formation model," *J. Sound Vib.*, **331**, 2558–2577 (2012).
[14] M. Miyamoto, Y. Ito, T. Iwasaki, T. Akamura, K. Takahashi, T. Takami, T. Kobayashi, A. Nishida and M. Aoyagi, "Numerical study on acoustic oscillations of 2D and 3D flue organ pipe like instruments with compressible LES," *Acta Acust. united Ac.*, **99**, 154–171 (2013).
[15] N. Giordano, "Direct numerical simulation of a recorder," *J. Acoust. Soc. Am.*, **133**, 1111–1118 (2013).
[16] N. Giordano, "Simulation studies of a recorder in three dimensions," *J. Acoust. Soc. Am.*, **135**, 906–916 (2014).
[17] H. Yokoyama, A. Miki, H. Onitsuka and A. Iida, "Direct numerical simulation of fluid-acoustic interactions in a recorder with tone holes," *J. Acoust. Soc. Am.*, **138**, 858–873 (2015).
[18] T. Kobayashi, T. Akamura, Y. Nagao, T. Iwasaki, K. Nakano, K. Takahashi and M. Aoyagi, "Interaction between compressible fluid and sound in a flue instrument," *Fluid Dyn. Res.*, **46**, 061411 (2014).
[19] K. Takahashi, S. Iwagami, T. Kobayashi and T. Takami, "Theoretical estimation of the acoustic energy generation and absorption caused by jet oscillation," *J. Phys. Soc. Jpn.*, **85**, 044402 (2016).
[20] C. Wagner, T. Hüttl and P. Sagaut, Eds., *Large-Eddy Simulation for Acoustics* (Cambridge University Press, New York, 2007).
[21] G. B. Brown, "The vortex motion causing edge tones," *Proc. Phys. Soc.*, **49**, 493–507 (1937).

APPENDIX: Numerical Simulation for the Short Flue Organ Pipe Studied by Ségoufin *et al.*

In this appendix, we shows numerical results for 2D models of the short flue organ pipe with and without chamfers studied by Ségoufin *et al.*, namely, the Short SgC model and the Short SgE model [8]. Figure A·1 shows the geometry of the foot chamber of the Short SgC model, which is almost the same as the 2D projection of the short flue organ pipe studied by Ségoufin *et al.* Figures A·2(a) and (b) show the pressure in the foot chamber compared with that in the pipe for the Short SgC model and the Short SgE model, respectively.

Comparing with the results in Fig. 7, it can be seen that the attack transients of these models are shorter than those of the LC and LE models and are almost the same time length as that of the SC model. The Short SgC model and the Short SgE model have the Helmholtz resonance frequencies 445 ± 5 Hz and 435 ± 5 Hz, which are slightly less than the oscillation frequencies 491 Hz and 508 Hz, respectively.

As shown in Fig. A·2(a) the oscillation amplitude for the Short SgC model is smaller than that of the Reference model and gradually fluctuates as a beat sound wave. The pressure oscillation in the foot chamber has almost the same frequency as that in the pipe, but they are not in

Fig. A·1 Geometry of the foot chamber of the Short Sg model with chamfers.

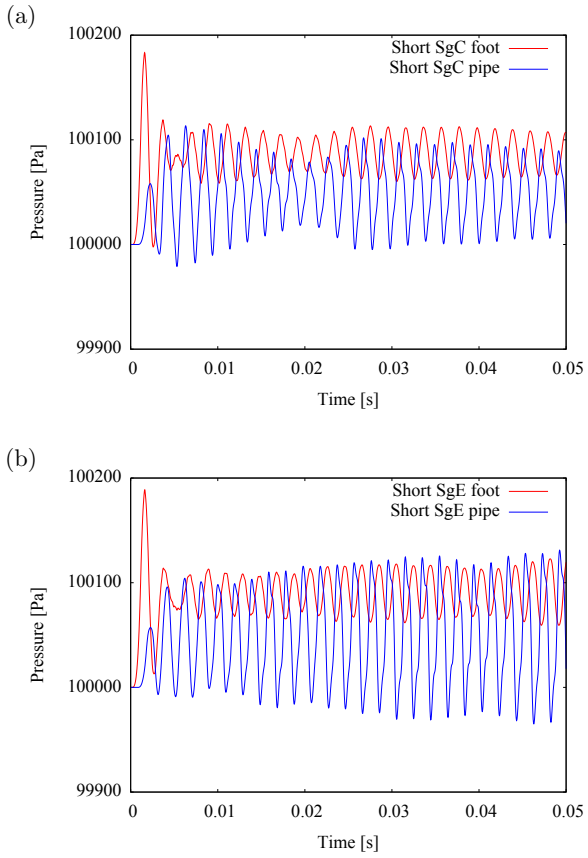

Fig. A·2 Pressure in the foot chamber and that in the pipe. (a) The Short Sg model with chamfers, i.e., Short SgC. (b) The Short Sg model without chamfers, i.e., Short SgE.

synchronization or anti-phase synchronization because the phase shift is not 0 or π.

As shown in Fig. A·2(b) the oscillation amplitude for the Short SgE model is slightly smaller than that of the SC model, but is larger than that of the Short SgC model. The pressure oscillation in the foot chamber has almost the same frequency as that in the pipe and they are nearly in anti-phase synchronization in the steady state. Thus, the oscillation of the model with chamfers is more unstable than that of the model without chamfers.

The wave forms observed for the Short SgC model and the Short SgE model are considerably deformed due to the effect of higher harmonics compared with that of the SC model. Therefore, our numerical calculation is qualitatively in agreement with the experimental result for the short flue organ pipe studied by Ségoufin *et al.*